ACES Asian Chemical Editorial Society

doi.org/10.1002/cnma.202200472

CHEMNANOMAT
Research Article

www.chemnanomat.org

Synthesis of Cationic Silver Nanoparticles with Highly Potent Properties against Oral Pathogens and Their Biofilms

Yanping He,[a, b] Don Hashan Kevin Ketagoda,[a, b] Richard Bright,[c] Susan Marie Britza,[a, b] Joshua Zechner,[a, b] Ian Musgrave,[a, b] Krasimir Vasilev,*[d] and Peter Zilm*[a, b]

Abstract: Dental caries is a major disease associated with the proliferation of acidogenic bacterial species such as *Streptococcus mutans* that are part of the commensal microbiota of the mouth. Silver nanoparticles (AgNPs) are attractive antibacterial agents as they target multiple sites in bacteria which reduces antimicrobial resistance. In this study, we synthesised stable, highly positively charged AgNPs capped with branched PEI (BPEI-AgNPs) and characterized them using UV–vis absorption, transmission electron microscopy (TEM), the size of which were approximately 7.5 nm. The antibacterial activity and anti-biofilm capacity of BPEI-AgNPs was investigated against cariogenic bacteria. Our results demonstrated that BPEI-AgNPs are potent clinical oral antiseptics. The cytotoxicity of the BPEI-AgNPs was also studied against two mammalian cell lines. The results indicated that BPEI-AgNPs were non-cytotoxic and were safer than commercially used dental antiseptics. We conclude that the BPEI-AgNPs are safe for oral clinical application and are an effective oral antimicrobial agent.

Introduction

As stated by the National Institutes of Health, most bacterial infections are associated with biofilms which account for 65% of microbial infections and approximately 80% of chronic infections.[1] Biofilms are characterized by a highly organized population of microbes embedded in an extracellular polymeric matrix.[2] During the initial formation of a biofilm, bacteria adhere and absorb to the extracellular polymeric substances which comprise of protein, extracellular DNA and polysaccharides.[3] The biofilm matrix is relatively impermeable to antibiotics and the sessile bacterial population is more resistant to antibacterial compounds compared to their planktonic counterparts.[4]

In the oral cavity, dental plaque is a typical example of a multispecies biofilm that attaches to pellicle, a glycoprotein layer that covers the tooth surface. Consisting of approximately 700 identified microbial species,[5] the diverse microbial residents all contribute to the complexity of the dental plaque community. A shift in the composition of dental plaque is known to cause the development of dental caries, which favours increasing levels of acidogenic and aciduric bacteria which includes members of the mutans Streptococci group including *Streptococcus mutans*.[6] *S. mutans* is a highly cariogenic bacterium responsible for the breakdown of enamel and dentin by producing lactic acid that demineralizes the inorganic component of teeth.[7] *S. mutans* are Gram-positive bacteria with the cytoplasmic membrane comprising of peptidoglycan layers with interwoven teichoic acids, which makes the bacterial cell wall negatively charged.[8]

Antibiotics have been commonly used to treat bacterial infections, but they often disturb the homeostasis of the commensal microbiome including those in digestive tract.[9] More significantly, there is a growing trend of pathogenic bacteria developing resistance against antibiotics.[10]

Chlorhexidine (CHX) has long been considered the gold-standard antimicrobial agent for oral use as a mouth wash, a concentration of 0.2% is regarded as the most effective.[11] However, adverse effects such as taste irritation, tooth staining, sore mouth and irritation of oral mucosa may limit its use.[12] Silver diamine fluoride (SDF) is most commonly used clinically for its high efficacy in arresting the progression of dental caries, but there is an aesthetic concern with staining the demineralised tissue black.[13]

Nanotechnology has been widely researched and used in numerous biomedical applications. Metallic nanoparticles including silver, gold, platinum show the most promising antibacterial and antiviral results, which can be attributed to their large surface-to-volume ratio and crystallographic surface structure.[14] Among these materials, silver nanoparticles (AgNPs) have attracted wide attention as they exhibit remarkable antimicrobial effect with low toxicity and cost.[15] Increasing research in AgNPs have been directed at dental applications

[a] Y. He, D. H. K. Ketagoda, S. M. Britza, J. Zechner, Dr. I. Musgrave, Ass. Prof. P. Zilm
Adelaide Dental School, University of Adelaide, Adelaide SA 5000 (Australia)
[b] Y. He, D. H. K. Ketagoda, S. M. Britza, J. Zechner, Dr. I. Musgrave, Ass. Prof. P. Zilm
Department of pharmacology, School of biomedicine, University of Adelaide, Adelaide SA 5000 (Australia)
[c] R. Bright
Academic Unit of STEM, University of South Australia, Mawson Lakes, SA 5095 (Australia)
[d] Prof. K. Vasilev
College of Medicine and Public Health, Flinders University, Bedford Park SA 5042 (Australia)
E-mail: peter.zilm@adelaide.edu.au

including restorative material,[16] implants,[17] and caries inhibitory solutions.[18] Significantly, when compared to the traditional antibiotics, silver nanoparticles have good bactericidal properties without leading to bacterial resistance.[19] Moreover, the anti-biofilm effect of AgNPs has also been demonstrated.[20] Comparative studies have also shown that nano silver shows reduced staining[13] of enamel and dentine compared to commercially available silver fluoride and silver diamine fluoride.[21]

The antibacterial activity of AgNPs is known to be highly related to factors such as size, shape, dose and surface charge.[22] It is widely recognised that smaller AgNPs (<10 nm) have significantly higher antimicrobial potency due to the greater surface area for silver ion release and more interactions with cell membranes.[23] Also, compared to negatively charged AgNPs, positively charged AgNPs have better antibacterial effect against Gram-positive bacteria.[20b,24]

Hence the aim of this study was to synthesise cationic AgNPs with high antibacterial and antibiofilm properties, while exhibiting low cytotoxicity to human mammalian cells. In accordance with this aim, low molecular weight branch polyethyleneimine (BPEI) (600 Da) was used as a capping agent to provide a positive charge to enable electrostatic interaction with the negatively charged bacterial surface. In addition, BPEI capped AgNPs were stabilized as the surface charge prevented their aggregation through electrostatic repulsion and steric hindrance.[25] It is widely accepted that the cytotoxicity of PEI is highly dependent on the molecular weight (MW) as low MW PEI shows a low cytotoxicity compared to high MW PEI.[26] PEI can be categorized into two groups based on the structure: linear PEI (LPEI) and branched PEI(BPEI). The difference is that BPEI has tertiary amino groups in addition to the primary and secondary amino groups, while LPEI possesses only the latter.[27] Given the above information, low MW BPEI was chosen for this study as it is safe and the tertiary amino groups enable higher steric and structural hindrance, which is important as it serves as capping agent for silver nanoparticles.

The antibacterial properties of the AgNPs were investigated against *S. mutans*, *Streptococcus sanguini*, *S. sobrinus* and *Actinomyces naeslundii* grown in a planktonic culture and as a multispecies biofilm grown on hydroxyapatite discs. Commercially available antibacterial agents were used for comparison. The cytotoxicity of the BPEI-AgNPs were evaluated against human gingival fibroblast to ensure biocompatibility. BPEI-AgNPs were shown to have excellent antibacterial and anti-biofilm properties at concentrations that displayed low cytotoxicity to human cells. We believe BPEI-AgNPs provide new options for treatment in clinical applications.

Results and Discussion

Synthesis and Characterizations of BPEI-AgNPs

The BPEI capped AgNPs were synthesized through a carefully tailored chemical reduction reaction that allows to improve size distribution and stability. The synthesis process is depicted in Figure 1. Briefly, $AgNO_3$ was used as precursor providing silver ions (Ag^+) and mixed with BPEI under ice-cold conditions. This was followed by the addition of $NaBH_4$, to reduce Ag^+ to its metallic form (Ag^0). BPEI is a synthetic cationic polymer, consisting of primary, secondary and tertiary amine groups, which can be protonated when ionized. During the synthesis process, the amine groups attached to the surface of metallic silver core via a metal ammine complex,[28] endowing a positive charge on the AgNP surface[29] as depicted in Figure 1.

ICP-MS was used to determine the concentration of BPEI-AgNP, which were ionized with HNO_3 (3% v/v) and then sorted and quantified (based on their mass to charge ratio) in the mass analyser. The concentration of BPEI-AgNP refers to total silver concentration, and the mass ratio of silver in BPEI-AgNP is around 10%.

BPEI-AgNPs were characterized using UV–vis spectroscopy, X-ray photoelectron spectroscopy, ZETA-sizer and transmission electron microscopy (TEM). The UV–Vis spectra in Figure 2(a) shows a single absorption peak at 400 nm, due to surface plasmon resonance occurring as the free electrons on the metal nanoparticle surface undergo collective oscillation in resonance with specific light wavelength. The results are in good agreement with previous studies.[30]

The TEM image in Figure 2b shows that the BPEI-AgNPs are spherical particles with an average size of 7.5 ± 0.09 nm (Fig-

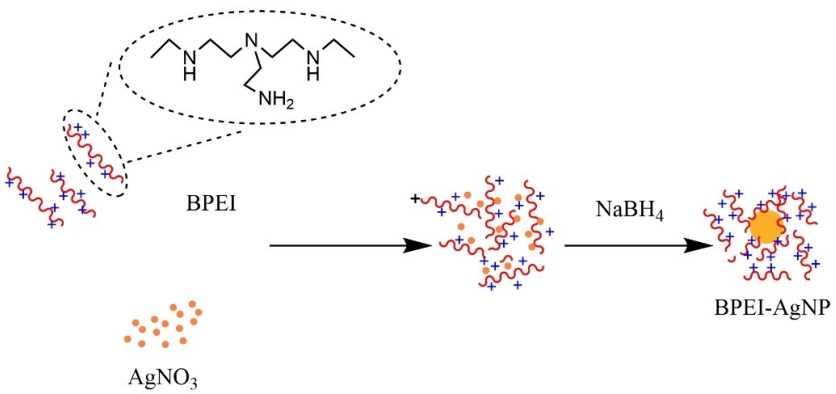

Figure 1. Schematic diagram of the BPEI-AgNPs synthesis with $NaBH_4$.

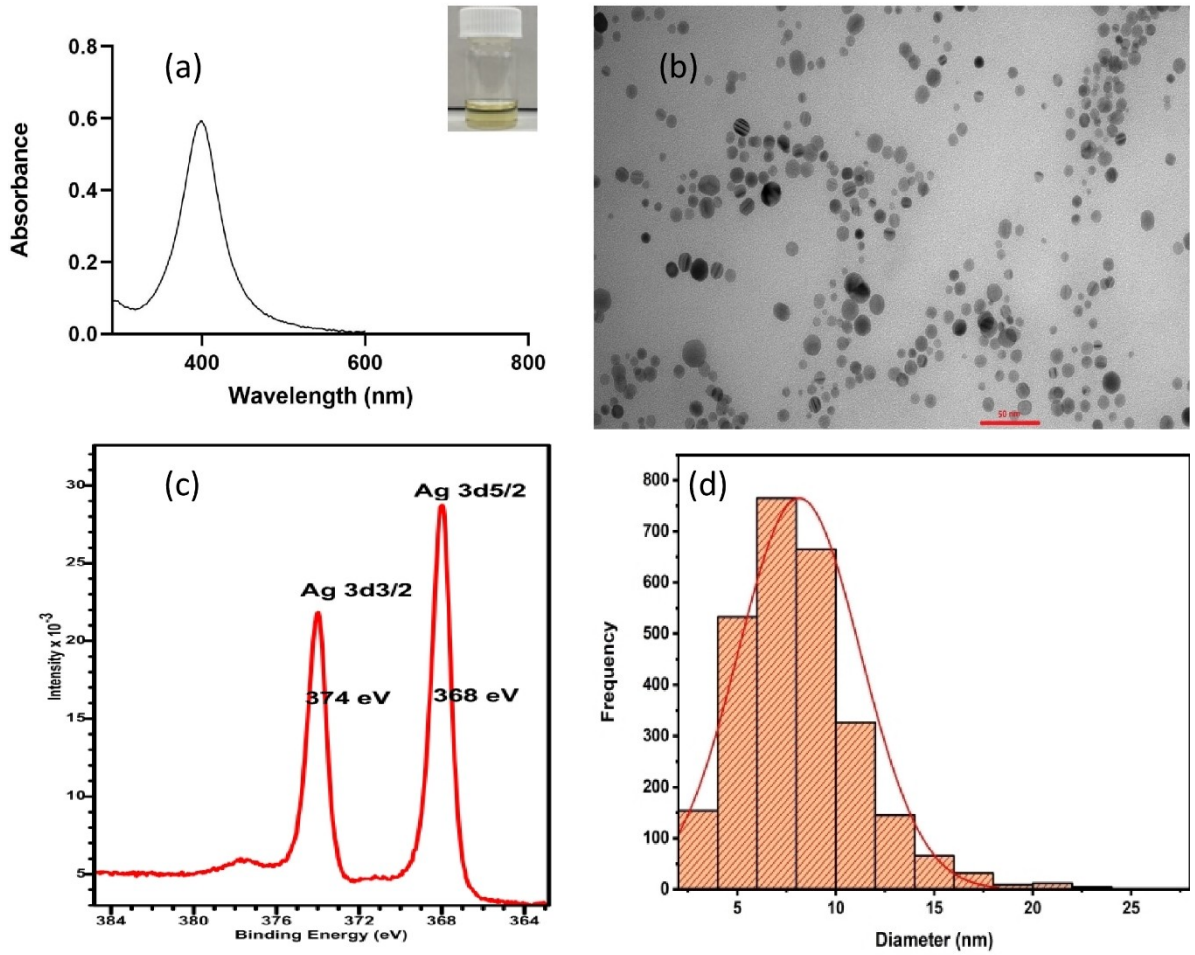

Figure 2. (a) UV–visible absorption spectra of BPEI-AgNPs. The inset (top right) is a representative image of the BPEI-AgNPs solution. (b) Representative TEM image of the BPEI-AgNPs. (c) High resolution XPS spectra for Ag3d. (d) Size distribution of BPEI-AgNPs after analysis using ImageJ and Origin.

ure 2d). The average ζ-potential of BPEI-AgNPs is +42 mV, indicating high stability for the colloidal. Zeta potential is widely used as indicator of the colloidal stability for NP dispersions, and it is noteworthy that for particles with ζ-potential values greater than +30 mV or more negative than −30 mV are considered stable dispersion.[31]

X-ray photoelectron spectroscopy was used to elucidate the chemical state of the BPEI-AgNPs. High resolution XPS (HR-XPS) in Figure 2(c) reveals the binding energy (BE) associated with the Ag 3d core level of the sample. The two spin-orbit pairs with binding energies at 368 and 374 eV respectively can be attributed to Ag 3d5/2 and Ag 3d3/2,[32] corresponding to metallic silver, which indicates the chemical reduction of $AgNO_3$ to Ag nanoparticles.

Minimum Inhibitory Concentration (MIC) and Minimum Bactericidal Concentration (MBC) Evaluation

The antibacterial activity of BPEI-AgNPs was determined against *S. mutans and S. sobrinus*. Using a broth microdilution method, after 24 h incubation under aerobic conditions at 37 °C, no turbidity was observed in the wells inoculated with 5 to 10 μg/ml BPEI-AgNPs indicating inhibition of bacteria growth. The suspension in all the wells were plated on TSB agar plates and incubated for 24 h. No growth was observed at a concentration of 10 μg/ml BPEI-AgNPs confirming this being the bactericidal concentration. Thus, the MIC/MBC of BPEI-AgNPs were 5 μg/ml, and 10 μg/ml respectively. BPEI was prepared in ten times the concentration of silver nanoparticles (e.g. 50 ug/mL, 100 ug/mL and 150 ug/mL), no inhibition was found. AgNP by itself was synthesised according to literature[33] for the antibacterial effect comparison, the results were summarized in Table 1, MIC was found in the concentrations of 10 to 15 ug/mL, but MBC was not detected in this concentration range, suggesting enhanced antibacterial effect after BPEI modification.

Biofilm eradication by BPEI-AgNPs

Confocal laser scanning microscopy (CLSM) was used for assessment of the effect of BPEI-AgNPs on biofilm eradication.

Table 1. MIC/MBC of AgNP and BPEI-AgNP (ug/ml) against oral pathogenic bacteria.

	AgNP		BPEI-AgNP	
	MIC	MBC	MIC	MBC
S. mutans	10	nd	5	10
S. sobrinus	10	nd	5	10

*nd: not detected.

In this study, four dental bacteria species including *S. mutans, S. sanguinis, S. sobrinus*, and *A. naeslundii* were chosen. Dental plaque is a complex biofilm formed on human tooth surface by oral bacteria, especially *S. mutans* and *S. sobrinus*, which are the major causative agents as they are associated with the synthesis of an extracellular capsule during fermentation of sucrose.[34] *S. sanguinis* is an early colonizer and plays a key role in biofilm development assisting the attachment of the succeeding organisms.[35] *A. naeslundii* inhabits the inner part of the biofilm, also participating in the initial stage of biofilm development.[36] To ensure sufficient coverage of biofilm on the HA discs, a multispecies biofilm was grown for 48 h. BPEI is well documented for its own antibacterial effect due to its ability to permeate and disrupt bacterial cell membranes,[37] thus BPEI at the final concentration in the nanoparticle colloidal (2 mg/mL) was used to treat biofilms to see if there was any impact on the biofilm. Chlorhexidine (CHX) is recognized as a "gold standard" antiplaque agent[38] and is commercially available at the concentration of 0.2%.[39] AgF solution is also commercially available (Riva Star Aqua) and is as effective in arresting caries as silver diamine fluoride,[40] thus both of CHX and AgF were used as positive controls.

The confocal microscopy images presented in Figure 3 were analysed using Imaris 3D/4D 260 image visualization and analysis software to illustrate bacterial cell viability. No significant difference in the cell viability was observed between 0.2% CHX and the BPEI-AgNPs treated groups across all the concentrations ranging from 10 μg/ml to 40 μg/ml. Bacterial viability on the disc surface for BPEI-AgNPs treated groups were reduced to only 19% at 10 μg/mL, 23% at 20 μg/mL and 20% at 40 μg/mL compared to 0.2% CHX (23%). In addition, BPEI-AgNPs had similar potency in killing biofilm cells to AgF (40 μg/ml), which reduced the bacterial viability to 26%. In comparison, kanamycin, at a concentration of 1.45 mg/mL, only reduced bacterial viability in the biofilm to 53%. The BPEI alone showed no antibiofilm effect with bacterial viability similar to the control at 80%. The confocal images presented in Figure 3B–H demonstrate the strong reduction in biovolume of BPEI-AgNPs were greater than CHX and kanamycin and comparable with AgF. The majority of bacterial cells in the untreated control and BPEI treated group (Figure 3(B) & (C)) were predominantly stained green, suggesting cells were viable, bacterial cells stained red or yellow indicate dead or dying cells.

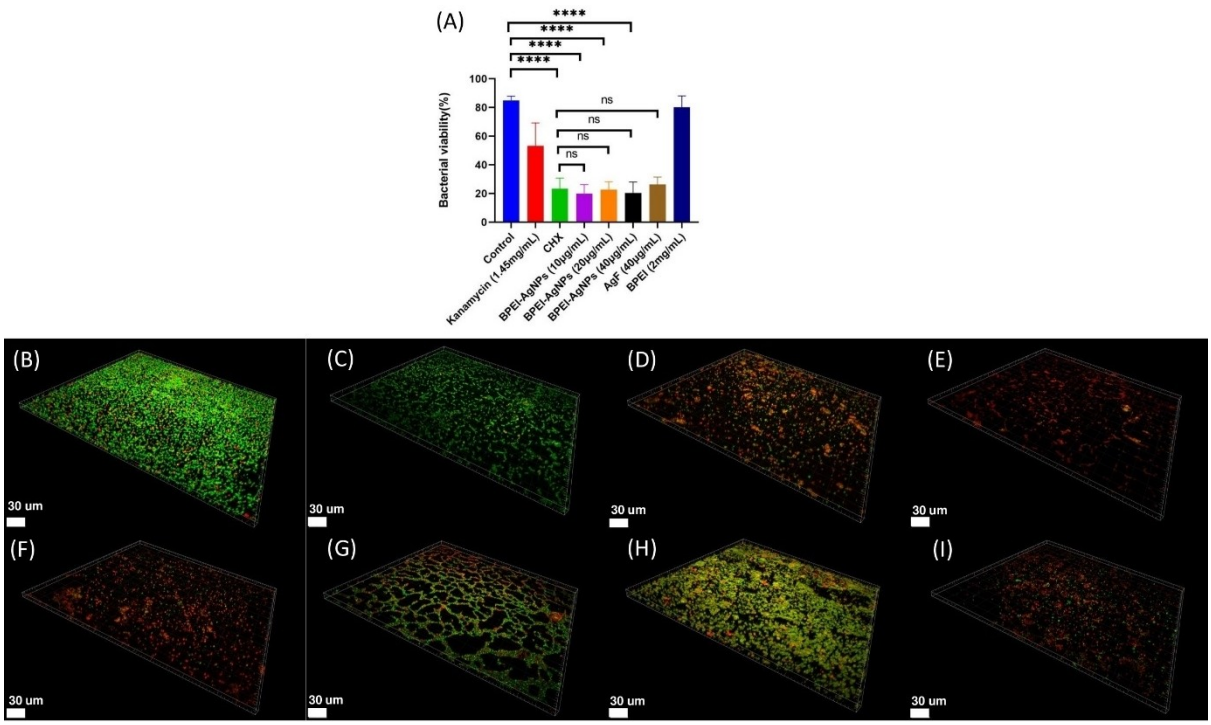

Figure 3. Evaluation of the antibiofilm effect of BPEI-AgNPs on a multispecies biofilm grown on hydroxyapatite. Bacterial cell viability for all groups (A). CLSM images of untreated multispecies biofilm (B), 2 mg/mL of BPEI treated biofilm (C), 10 μg/mL of BPEI-AgNPs treated biofilm (D), 20 μg/mL of BPEI-AgNPs treated biofilm (E), 40 μg/mL of BPEI-AgNPs treated biofilm (F), 1.45 mg/mL of kanamycin treated biofilm (G), 0.20% CHX treated biofilm (H) and 40 μg/mL of AgF treated biofilm (I). Data are shown as (mean ± SD; n = 6); the **** denotes significant difference compared to the control and ns denotes no significant difference compared to 0.2% CHX using one-way ANOVA followed by Dunnett's multiple comparison test. *$P < 0.05$, **$P < 0.01$, ***$P < 0.001$ and ****$P < 0.0001$.

Evaluation of cytotoxicity of BPEI-AgNPs

In addition to their excellent antibacterial and antibiofilm effect, it was important to evaluate the possible toxicity of BPEI-AgNPs on mammalian cells. To study the potential cellular cytotoxicity, we conducted an *in-vitro* cell viability assay against primary human gingival fibroblast (HGF) and human colorectal adenocarcinoma (Caco-2) cells. Oral fibroblasts like HGF are considered biologically relevant for biocompatibility study as they are the main component of gingival tissue,[41] and differentiated Caco-2 cells are more representative of intestinal cells with multiple intestinal functions.[42] Considering potential future oral application, these two related cell lines were selected.

As shown in Figure 4, there was no significant difference in cell viability between the control and BPEI-AgNPs treated cells in the concentration range of 5–15 μg/ml. Significantly, 15 μg/ml was 3 times the MIC concentration used on bacteria and is considered a nontoxic concentration by the International Standard ISO 2009 "Biological evaluation of medical devices".[43] However, when the concentration increased to 20 μg/mL, cell viability decreased to approximately 9% in both cell lines, indicating this concentration to be significantly cytotoxic. Importantly, the same cytotoxic effect was also observed with AgF (20 μg/mL), with cell viability of only 7.52% in HGF and 8.25% in differentiated Caco-2. BPEI-AgNPs at 10 μg/mL, which is the minimum bactericidal concentration (MBC) for planktonic bacterial cells and were effective in eliminating a multispecies biofilm, also showed no cytotoxicity to both cell lines. BPEI at 2 mg/mL had no cytotoxicity on either cell line, which is in line with other literature that low molecular weight PEI has less cytotoxicity,[44] and branch PEI is even less toxic compared to linear PEI.[27b] It is important to note that commercially used 0.2% CHX decreased cell viability to 12% for differentiated Caco-2 and 16% for HGFs. This result suggests that our BPEI-AgNPs when used in effective concentration range of 5–15 μg/ml might be safer than some commercially available products.

Published literature have shown that AgNPs are inevitably accompanied by cytotoxicity to several cell lines.[45] While there is no consensus on the underlying mechanism for the toxicity of AgNPs, many have suggested the release of Ag ions,[46] interaction with mitochondria and production of reactive oxygen species (ROS) induces apoptosis.[45b,47] Moreover, the size effect of AgNPs is an important factor, small AgNPs were reported to be more toxic than larger ones, as they have larger surface area and release silver ions faster, leading to a higher toxicity.[48] Our synthesised BPEI-AgNPs, however, showed excellent antibacterithanal and antibiofilm effects at a low concentration without nanotoxicity toward two related mammalian cell lines, which makes them a potential therapeutic agent for future clinical use.

Conclusions

We have developed small cationic branched PEI stabilised AgNPs of size of ~7.5 nm that possess excellent antimicrobial properties against both oral planktonic cells and multispecies biofilms. The BPEI-AgNPs potency can be ascribed to their small size and positive charge which provides better interaction with bacteria cells due to enhanced electrostatic attraction. Further to that, BPEI-AgNPs were shown to be as effective as CHX and silver fluoride in reducing and destabilising multispecies biofilms while potentially overcoming the irritation (CHX) and staining issue (AgF). In addition, we have demonstrated their good biocompatibility with two cell lines at a concentration three times the MIC of BPEI-AgNPs that the nanoparticles may be less cytotoxic than CHX. The results of this work suggest that BPEI-AgNPs may be an alternative to currently used oral antiseptics and have future as an oral antimicrobial agent in clinical applications.

Experimental Section

Materials

$AgNO_3$ (99.99%), sodium borohydride (NaBH4), branch polyethylenimine (MW = 600) were purchased from Sigma–Aldrich (Sydney, Australia). Sodium hydroxide (NaOH) from chem supply and acetic acid from UNIVAR were analytical grade. Tryptone soya broth (TSB) was purchased from Oxoid Ltd. (Basingstoke, UK).

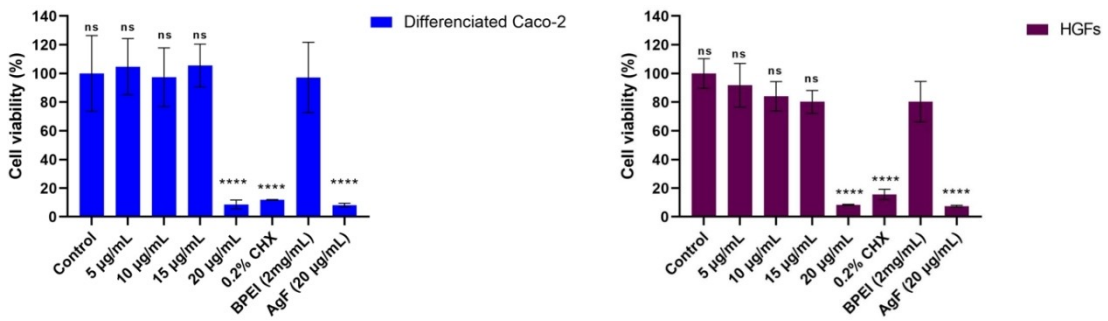

Figure 4. Cytotoxicity of BPEI-AgNPs (at different concentrations), 0.2% CHX and BPEI (2 mg/mL) on differentiated Caco-2 and HGFs after 24 h exposure. The cell viability was given as a percentage and normalized to the control (mean ± SD; n = 6); ns denotes no significant difference, and * denotes significant difference compared to the control ($p < 0.05$) using Two-way ANOVA followed by Dunnett's multiple comparison test. *$P < 0.05$, **$P < 0.01$, ***$P < 0.001$ and ****$P < 0.0001$.

Synthesis of BPEI-AgNPs

Branched PEI (MW = 600) was dissolved completely in deionized water to a final concentration of 16 mg/mL and the pH was adjusted to 6.8 with acetic acid (pH 2.0). Subsequently, 1 ml of an aqueous silver nitrate ($AgNO_3$, Sigma–Aldrich, MI, USA) solution (20 mM) and 1 mL of the prepared BPEI solution was mixed with 6 mL of deionized water under vigorous stirring in an ice bath for 15 min. 35 μL of the freshly prepared $NaBH_4$ (Sigma–Aldrich, MI, USA) solution (45 mM) was then added to the mixture in a dropwise manner followed by continuous stirring at 1100 rpm for 2 days. The slow colour-change from light to brown yellow indicated the formation of BPEI-AgNP. After synthesis, the BPEI-AgNP suspension was centrifuged at 10000 g for 3 min, supernatant was taken out and kept in fridge for further use.

Characterization of BPEI-AgNPs

The UV absorbance spectra of the BPEI-AgNP solution were measured using UV–vis spectroscopy (NanoDrop 2000c, Thermo-Fisher Scientific, USA) The zeta-potential of the BPEI-AgNP was measured using Malvern Zetasizer Nano (Malvern Panalytical, Malvern, UK). The size and morphology of AgNPs were imaged by high resolution transmission electron microscopy (TEM) (Tecnai G2, FEI Company, OR, USA) at 120 kV. In brief, 5 μL of BPEI-AgNP solution was dropped on to the carbon-coated copper grid and dried at room temperature. The AgNP size distribution was determined based on analysing over 2000 nanoparticles using ImageJ software version v1.53d (NIH, USA). Total metal concentrations were determined using inductively coupled mass spectroscopy (ICP-MS) after sample digestion with HNO3 (3% v/v).

High resolution X-ray photoelectron spectroscopy (XPS) analysis

XPS spectra were measured using AXIS Ultra DLD (Kratos Analytical, Manchester, U.K.) with a monochromatic Al Ka radiation source (1486.6 eV) and operated at a power of 225 W. High resolution (0.1 eV) spectra were recorded to analyse the chemical states of silver (pass energy of 20 eV). Calibration of all binding energies were carried out by assigning the C1s carbon peak a binding energy of 285 eV. 480 CASA XPS software was used for spectra analysing and component fitting.

Cell lines and culture conditions

Human colon adenocarcinoma cell line Caco-2 was a generous gift of Dr Scott Smid (catalogue no. ATCC HTB-37, American Type Culture Collection, Manassas, VA, USA), and the human gingival fibroblasts (HGFs) were primary cell lines obtained from patient from the third molar region with informed consent at University of Adelaide (Approval Number H-112-2008). Caco-2 cells and HGFs passages were cultured in Dulbecco's modified Eagle's medium (DMEM) supplemented with 10% (v/v) foetal bovine serum (FBS) and1% (v/v) penicillin/streptomycin and incubated at 37 °C, 5% CO_2 in a humidified atmosphere of. Cells were grown to 70–80% confluency prior to seeding into 96 well plates at 1×10^5 cells per well. Caco-2 cells were further grown for differentiation according to published literature with minor modification[49] in 96-well plates for 10 days, and growth medium was changed every 2 days.

In Vitro Antibacterial Evaluation of BPEI-AgNPs

Bacterial Strains and Culture

S. sobrinus (ATCC 33478) and *S. mutans* Ingbritt strain[50] were streaked onto Tryptone soya broth (TSB) agar plates from frozen stock cultures kept in 40% glycerol at −80 °C. A single colony of each bacterial strain was inoculated into fresh TSB and cultured overnight at 37 °C.

Determination of Minimal inhibitory concentration (MIC) and Minimum bactericidal concentration (MBC)

The MIC and MBC against *S. mutans* and *S. sobrinus* were determined using a broth microdilution method according to CLSI- and EUCAST-Standards[51] with minor modifications. Briefly, each bacterium was grown as described above, and upon reaching mid-log phase was subsequently diluted with TSB to 10^7 CFU/mL based on the optical density at 600 nm (OD_{600}). Then, 180 μL of the diluted aliquots (in TSB) of the BPEI-AgNPs were added to the wells of a 96-well plate and inoculated with 20 μL of the diluted *S. mutans* or *S. sobrinus* to give a final concentration of 1×10^6 CFU/mL. Sterile TSB served as blank, bacterial suspensions without BPEI-AgNPs served as the positive control and Kanamycin (1.45 mg/mL) as the negative control. Each experiment was conducted in triplicate for all groups. The 96 well plate was then incubated at 37 °C for 24h, and the OD_{600} was measured using a Synergy HTX multi-mode reader (BioTek, VT, USA). The MIC was the lowest concentration of BPEI-AgNPs used to inhibit visible growth after incubation. MBC was determined by pipetting 5 μL of culture from wells with no visible growth, and plating onto a TSB-agar plate. The MBC was defined as the lowest concentration of BPEI-AgNPs that produced no bacterial growth on the plate after overnight incubation at 37 °C.

Multispecies Biofilm Model

Sterile hydroxyapatite (HA) disks (5 mm diameter by 2 mm thickness; Clarkson Chromatography Products, PA, USA) were used as the substrate for biofilm growth. In brief, sterile hydroxyapatite (HA) discs were placed in a 24 well plate with 1.5 ml of bacterial suspension containing *S. mutans*, *S. sanguinis* P_4A_7,[52] *S. sobrinus* and *A. naeslundii* (ATCC 19039) at a final density of 1×10^6 CFU ml^{-1} for each strain. After incubation for 48 h at 37 °C the growth medium was replaced with either, BPEI-AgNPs ranging from 0–40 μg/mL, 1.45 mg/mL of kanamycin, 0.20% chlorhexidine and 40 μg/mL of silver fluoride (AgF), 2 mg/ml of BPEI and plates were incubated at 37 °C. After 24 h, the HA discs were rinsed with phosphate buffered saline (PBS, pH 7.4) to remove unattached bacteria. HA discs were then used for viability and qualitative analysis of the biofilm.

Evaluation of Biofilm with Confocal Laser Scanning Microscopy (CLSM)

LIVEDEAD® BacLight™ viability kit (Invitrogen, ThermoFisher Scientific, MA, USA) containing two dyes, SYTO 9 stain and propidium iodide (PI), was prepared according to manufacturer's protocols and applied to the biofilm on HA discs. The discs were covered and incubated at room temperature for 20 minutes, protected from light before discs were inverted onto a clean coverslip and imaged using an Olympus FV3000 CLSM (Olympus, Tokyo, Japan).

Three random spots on the HA disc were imaged and the results averaged. Confocal images were processed using the Imaris v7.2 software (Bitplane Inc., MN, USA), and cell viability was determined.

Cytotoxicity Studies

The cytotoxicity of BPEI-AgNPs was determined using 3-(4, 5-dimethylthiazol-2-yl)-2, 5-diphenyltetrazolium bromide (MTT) assay on a human gingival fibroblast (HGF) cell line and differentiated Caco-2 cells. HGF and differentiated Caco-2 cells were cultured as per the procedure mentioned previously. HGFs were seeded into 96-well plates at 1×10^5 cells per well with 10% FBS DMEM and incubated for 48 h prior to testing, Caco-2 cells were seeded at the same concentration and allowed to differentiate before testing. When cells reached confluency, growth media was discarded and cells were then exposed to a series of BPEI-AgNPs solutions with concentration ranging from 0 to 40 ug/mL in DMEM and 0.2% CHX as the positive control. 96-well plates were then incubated for 24 hours. Growth media was then discarded and replaced with serum-free DMEM containing 0.25 mg/ml MTT. The viable cells with intact mitochondria reduce MTT to insoluble purple formazan. Plates were incubated for a further 4 h, then the media was discarded and DMSO was added to dissolve the insoluble formazan. Absorbance of the samples were measured at 570 nm using Synergy HTX multi-mode reader (BioTek, VT, USA).

Acknowledgements

PZ thanks the Australian Dental Research Foundation for project grant (353-2018). YH acknowledges the financial support from Australian Government Research Training Program Scholarship. The authors are thankful to Victor Marino for technical assistance and technical assistance at Adelaide Microscopy, the University of Adelaide, a facility that is funded by the University and State and Federal Governments. The authors also acknowledge the facilities, scientific and technical assistance of Microscopy Australia at the University of South Australia, a facility that is co-funded by the University of South Australia, the State and Federal Governments. KV thanks NHMRC for Fellowship GNT1194466. Open Access publishing facilitated by The University of Adelaide, as part of the Wiley - The University of Adelaide agreement via the Council of Australian University Librarians.

Conflict of Interest

The authors declare no conflict of interest.

Data Availability Statement

The data that support the findings of this study are available from the corresponding author upon reasonable request.

Keywords: Antibiofilm · Branch polyethylenimine · Chlorhexidine. Dental caries · Silver nanoparticle

[1] a) S. Medici, M. Peana, V. M. Nurchi, M. A. Zoroddu, *J. Med. Chem.* **2019**, *62*, 5923–5943; b) NIH, *National Institute of Health* **2002**.
[2] C. Goller, T. Romeo, *Bacterial Biofilms* **2008**, 37–66.
[3] a) H.-C. Flemming, J. Wingender, *Nat. Rev. Microbiol.* **2010**, *8*, 623–633; b) I. W. Sutherland, *Trends Microbiol.* **2001**, *9*, 222–227.
[4] a) T.-F. Mah, *Future Microbiol.* **2012**, *7*, 1061–1072; b) U. Römling, C. Balsalobre, *J. Intern. Med.* **2012**, *272*, 541–561.
[5] F. E. Dewhirst, T. Chen, J. Izard, B. J. Paster, A. C. Tanner, W.-H. Yu, A. Lakshmanan, W. G. Wade, *J. Bacteriol.* **2010**, *192*, 5002–5017.
[6] S. Dashper, E. Reynolds, *J. Dent. Res.* **1992**, *71*, 1159–1165.
[7] M. Aqawi, R. V. Sionov, R. Gallily, M. Friedman, D. Steinberg, *Front. Microbiol.* **2021**, *12*.
[8] a) E. E. Fröhlich, E. Fröhlich, *Int. J. Mol. Sci.* **2016**, *17*, 509; b) Y. N. Slavin, J. Asnis, U. O. Häfeli, H. Bach, *J. Nanobiotechnol.* **2017**, *15*, 1–20.
[9] a) Z. Lu, K. Rong, J. Li, H. Yang, R. Chen, *J. Mater. Sci. Mater. Med.* **2013**, *24*, 1465–1471; b) L. Espinosa-Cristóbal, G. Martínez-Castañón, R. Martínez-Martínez, J. Loyola-Rodriguez, N. Patino-Marin, J. Reyes-Macias, F. Ruiz, *Mater. Lett.* **2009**, *63*, 2603–2606.
[10] a) H. Altman, D. Steinberg, Y. Porat, A. Mor, D. Fridman, M. Friedman, G. Bachrach, *J. Antimicrob. Chemother.* **2006**, *58*, 198–201; b) M. K. Rai, S. Deshmukh, A. Ingle, A. Gade, *J. Appl. Microbiol.* **2012**, *112*, 841–852.
[11] C. G. Jones, *Periodontol. 2000* **1997**, *15*, 55–62.
[12] P. James, H. V. Worthington, C. Parnell, M. Harding, T. Lamont, A. Cheung, H. Whelton, P. Riley, *Cochrane Database Syst. Rev.* **2017**.
[13] S. Tirupathi, S. Nirmala, S. Rajasekhar, S. Nuvvula, *J. Clin. Exp. Dent.* **2019**, *11*, e105.
[14] a) M. Oves, M. Aslam, M. A. Rauf, S. Qayyum, H. A. Qari, M. S. Khan, M. Z. Alam, S. Tabrez, A. Pugazhendhi, I. M. Ismail, *Mater. Sci. Eng. C.* **2018**, *89*, 429–443; b) M. S. Samuel, S. Jose, E. Selvarajan, T. Mathimani, A. Pugazhendhi, *J. Photochem. Photobiol. B* **2020**, *202*, 111642.
[15] a) S. Xiao, H. Wang, K. Liang, F. Tay, M. D. Weir, M. A. S. Melo, L. Wang, Y. Wu, T. W. Oates, Y. Ding, *J. Dent.* **2019**, *81*, 17–26; b) H. Haidari, N. Goswami, R. Bright, Z. Kopecki, A. J. Cowin, S. Garg, K. Vasilev, *Nanoscale Adv.* **2019**, *1*, 2365–2371.
[16] H. Jia, W. Hou, L. Wei, B. Xu, X. Liu, *Dent. Mater.* **2008**, *24*, 244–249.
[17] F. A. Sheikh, N. A. Barakat, M. A. Kanjwal, R. Nirmala, J. H. Lee, H. Kim, H. Y. Kim, *J. Mater. Sci. Mater. Med.* **2010**, *21*, 2551–2559.
[18] E. Swift Jr, *J. Dent. Res.* **1989**, *68*, 1088–1093.
[19] A. Panáček, M. Smékalová, R. Večeřová, K. Bogdanová, M. Röderová, M. Kolář, M. Kilianová, Š. Hradilová, J. P. Froning, M. Havrdová, *Colloids Surf. B. Biointerfaces* **2016**, *142*, 392–399.
[20] a) M. Radzig, V. Nadtochenko, O. Koksharova, J. Kiwi, V. Lipasova, I. Khmel, *Colloids Surf. B. Biointerfaces* **2013**, *102*, 300–306; b) H. Haidari, R. Bright, Z. Kopecki, P. S. Zilm, S. Garg, A. J. Cowin, K. Vasilev, N. Goswami, *ACS Appl. Mater. Interfaces* **2021**; c) H. Haidari, Z. Kopecki, R. Bright, A. J. Cowin, S. Garg, N. Goswami, K. Vasilev, *ACS Appl. Mater. Interfaces* **2020**, *12*, 41011–41025.
[21] L. Espíndola-Castro, A. Rosenblatt, A. Galembeck, G. Monteiro, *Oper. Dent.* **2020**, *45*, 435–441.
[22] a) T. C. Dakal, A. Kumar, R. S. Majumdar, V. Yadav, *Front. Microbiol.* **2016**, *7*, 1831; b) X. Hong, J. Wen, X. Xiong, Y. Hu, *Environ. Sci. Pollut. Res. Int.* **2016**, *23*, 4489–4497; c) M. A. Raza, Z. Kanwal, A. Rauf, A. N. Sabri, S. Riaz, S. Naseem, *Nanomaterials* **2016**, *6*, 74.
[23] a) L. Shang, K. Nienhaus, G. U. Nienhaus, *J. Nanobiotechnol.* **2014**, *12*, 1–11; b) S. Agnihotri, S. Mukherji, S. Mukherji, *RSC Adv.* **2014**, *4*, 3974–3983.
[24] A. Abbaszadegan, Y. Ghahramani, A. Gholami, B. Hemmateenejad, S. Dorostkar, M. Nabavizadeh, H. Sharghi, *J. Nanomater.* **2015**, *2015*.
[25] L. Malassis, R. Dreyfus, R. J. Murphy, L. A. Hough, B. Donnio, C. B. Murray, *RSC Adv.* **2016**, *6*, 33092–33100.
[26] a) K. Morimoto, M. Nishikawa, S. Kawakami, T. Nakano, Y. Hattori, S. Fumoto, F. Yamashita, M. Hashida, *Mol. Ther.* **2003**, *7*, 254–261; b) D. Fischer, T. Bieber, Y. Li, H.-P. Elsässer, T. Kissel, *Pharm. Res.* **1999**, *16*, 1273–1279.
[27] a) X. Gao, L. Yao, Q. Song, L. Zhu, Z. Xia, H. Xia, X. Jiang, J. Chen, H. Chen, *Biomaterials* **2011**, *32*, 8613–8625; b) V. Kafil, Y. Omidi, *Bioimpacts.* **2011**, *1*, 23.
[28] S. Kobayashi, K. Hiroishi, M. Tokunoh, T. Saegusa, *Macromolecules* **1987**, *20*, 1496–1500.
[29] S. Tan, M. Erol, A. Attygalle, H. Du, S. Sukhishvili, *Langmuir* **2007**, *23*, 9836–9843.
[30] a) Y. Zhang, H. Peng, W. Huang, Y. Zhou, X. Zhang, D. Yan, *J. Phys. Chem. C* **2008**, *112*, 2330–2336; b) Z. Liu, Z. Xing, Y. Zu, S. Tan, L. Zhao, Z. Zhou, T. Sun, *Mater. Sci. Eng. C.* **2012**, *32*, 811–816.

[31] M. Meléndrez, G. Cárdenas, J. Arbiol, *J. Colloid Interface Sci.* **2010**, *346*, 279–287.
[32] a) E. Sumesh, M. Bootharaju, T. Pradeep, *J. Hazard. Mater.* **2011**, *189*, 450–457; b) N. Goswami, R. Bright, R. M. Visalakshan, B. Biswas, P. Zilm, K. Vasilev, *Nanoscale Adv.* **2019**, *1*, 2356–2364.
[33] L. Mulfinger, S. D. Solomon, M. Bahadory, A. V. Jeyarajasingam, S. A. Rutkowsky, C. Boritz, *J. Chem. Educ.* **2007**, *84*, 322.
[34] M. Shemesh, A. Tam, D. Steinberg, *J. Med. Microbiol.* **2007**, *56*, 1528–1535.
[35] J. A. Aas, B. J. Paster, L. N. Stokes, I. Olsen, F. E. Dewhirst, *J. Clin. Microbiol.* **2005**, *43*, 5721–5732.
[36] I. Dige, M. Raarup, J. Nyengaard, M. Kilian, B. Nyvad, *Microbiology* **2009**, *155*, 2116–2126.
[37] a) M. Azevedo, P. Ramalho, A. Silva, R. Teixeira-Santos, C. Pina-Vaz, A. Rodrigues, *J. Med. Microbiol.* **2014**, *63*, 1167–1173; b) K. A. Gibney, I. Sovadinova, A. I. Lopez, M. Urban, Z. Ridgway, G. A. Caputo, K. Kuroda, *Macromol. Biosci.* **2012**, *12*, 1279–1289.
[38] K. Kour, S. Kaur, P. Singh, *Int. J. Oral Health Dent* **2019**, *5*, 97–103.
[39] E. K. Mauland, H. R. Preus, A. M. Aass, *J. Clin. Periodontol.* **2020**, *47*, 1522–1527.
[40] B. Turton, R. Horn, C. Durward, *Heliyon* **2020**, *6*, e04287.
[41] N. Wada, D. Menicanin, S. Shi, P. M. Bartold, S. Gronthos, *J. Cell. Physiol.* **2009**, *219*, 667–676.
[42] A. Lampen, A. Bader, T. Bestmann, M. Winkler, L. Witte, J. Borlak, *Xenobiotica* **1998**, *28*, 429–441.
[43] B. Iso, B. STANDARD, *Part* **2009**, *1*, 10993.
[44] W.-C. Hung, J.-Y. Cherng, *Polymer* **2015**, *7*, 2131–2145.
[45] a) S. Hussain, K. Hess, J. Gearhart, K. Geiss, J. Schlager, *Toxicol. in Vitro* **2005**, *19*, 975–983; b) Y.-H. Hsin, C.-F. Chen, S. Huang, T.-S. Shih, P.-S. Lai, P. J. Chueh, *Toxicol. Lett.* **2008**, *179*, 130–139; c) R. Foldbjerg, P. Olesen, M. Hougaard, D. A. Dang, H. J. Hoffmann, H. Autrup, *Toxicol. Lett.* **2009**, *190*, 156–162.
[46] C. Beer, R. Foldbjerg, Y. Hayashi, D. S. Sutherland, H. Autrup, *Toxicol. Lett.* **2012**, *208*, 286–292.
[47] C. Carlson, S. M. Hussain, A. M. Schrand, L. K. Braydich-Stolle, K. L. Hess, R. L. Jones, J. J. Schlager, *J. Phys. Chem. B* **2008**, *112*, 13608–13619.
[48] a) G. A. Sotiriou, S. E. Pratsinis, *Curr. Opin. Chem. Eng.* **2011**, *1*, 3–10; b) R. Shanmuganathan, D. MubarakAli, D. Prabakar, H. Muthukumar, N. Thajuddin, S. S. Kumar, A. Pugazhendhi, *Environ. Sci. Pollut. Res. Int.* **2018**, *25*, 10362–10370.
[49] L. Böhmert, B. Niemann, A. F. Thünemann, A. Lampen, *Arch. Toxicol.* **2012**, *86*, 1107–1115.
[50] D. Ellwood, I. Hamilton, *Infect. Immun.* **1982**, *36*, 576–581.
[51] a) E. C. o. A. S. Testing, *Version* **2015**, *5*, 2015; b) I. O. f. Standardization, *Clinical Laboratory Testing and in Vitro Diagnostic Test Systems-Susceptibility Testing of Infectious Agents and Evaluation of Performance of Antimicrobial Susceptibility Test Devices: Reference Method for Testing the in Vitro Activity of Antimicrobial Agents Against Rapidly Growing Aerobic Bacteria Involved in Infectious Diseases*, ISO, **2006**.
[52] A. H. Rogers, P. S. Zilm, N. J. Gully, A. L. Pfennig, *Curr. Microbiol.* **1990**, *20*, 19–22.

Manuscript received: October 19, 2022
Revised manuscript received: January 8, 2023
Accepted manuscript online: January 12, 2023
Version of record online: January 23, 2023